Asia Pacific Academy of Science Pte. Ltd.

Computer and Telecommunication Engineering 2024, 2(2), 2524.
https://doi.org/10.54517/cte.v2i2.2524

Article

Analyzing the performance of secondary users in satellite-terrestrial systems with cognitive radio assistance

Huu Q. Tran

Faculty of Electronics Technology (FET), Industrial University of Ho Chi Minh City (IUH), Ho Chi Minh City 700000, Vietnam; tranquyhuu@iuh.edu.vn

CITATION

Tran HQ. Analyzing the performance of secondary users in satellite-terrestrial systems with cognitive radio assistance. Computer and Telecommunication Engineering. 2024; 2(2): 2524. https://doi.org/10.54517/cte.v2i2.2524

ARTICLE INFO

Received: 29 January 2024
Accepted: 20 May 2024
Available online: 17 June 2024

Abstract: The paper investigates the outage probability (OP) of a cognitive radio-based satellite-ground transmission system. In this configuration, both direct and relay links are activated to facilitate transmission from the primary satellite source to terrestrial users. The primary metric under scrutiny is the outage probability for both the primary and secondary networks. Utilizing the Shadowed-Rician fading model, commonly applied to satellite channels, for the satellite segment, and Nakagami-m fading models for terrestrial channels, we assess the OP by analyzing the expressions for both primary and secondary users. Additionally, we explore the impact of key system parameters on the OP's performance. Indeed, the signal-to-noise ratio (SNR) and target rate are the main factors affecting the outage behavior of users on the ground. We identify certain conditions necessary to achieve improved performance by controlling key system parameters. Furthermore, this paper provides guidelines for designing cognitive radio (CR) systems in satellite configurations to meet the quality requirements of received signals on the ground. The analysis results are validated through Monte Carlo simulations implemented using MATLAB.

Keywords: cognitive radio (CR); outage probability (OP); satellite-terrestrial system

1. Introduction

In recent times, a novel and promising network paradigm referred to as the Hybrid Satellite-Terrestrial Relay Network (HSTRN) system has emerged, as elucidated in recent publications [1–4]. This innovative system ingeniously combines the capabilities of both satellite and terrestrial networks, presenting a hybridized architecture that holds significant potential for transformative advancements in the realm of mobile communications. The distinctive feature of HSTRN systems lies in their ability to facilitate collaboration between terrestrial relays and satellite mobile communications [5].

The HSTRN offers a myriad of advantages, particularly benefiting portable and mobile users by providing efficient broadcast and multicast services. This proves advantageous in scenarios requiring indoor coverage, especially in environments with significant obstacles such as shopping malls and tunnels, where non-line-of-sight (NLOS) communications are crucial for seamless connectivity. HSTRN also proves to be beneficial for relaying networks through the integration of amplify-and-forward (AnF) [6–10] and decode-and-forward (DnF) relaying [11–13]. The application of amplify-and-forward (AnF) relaying involves the relay amplifying the received signal before forwarding it, enhancing signal strength and overall communication efficiency. Similarly, decode-and-forward (DnF) relaying entails the relay decoding the received signal, re-encoding it, and then forwarding it to the destination, contributing to improved reliability and data integrity. In an extension of prior research, Hemachandra and Beaulieu [14] delved into a multiuser relay network case within the HSTRN framework. This configuration allows a relay to play a pivotal role in assisting signal transmission between multiple users and a source node, showcasing the adaptability and versatility of HSTRN in supporting complex communication scenarios.

The incorporation of functionalities for the HSTRN is facilitated through the introduction of IEEE 802.11s and IEEE 802.16j standards [15]. These standards play a crucial role in defining and standardizing the operational aspects of HSTRN, ensuring seamless integration into existing communication frameworks.

As the demand for high-throughput services catering to a large number of terrestrial users becomes paramount in the development of 5G mobile systems, the exploration of various applications within the HSTRN context gains significance [16,17]. The HSTRN framework proves to be highly adaptable and conducive to addressing the evolving needs of modern communication systems.

In the pursuit of achieving multiuser diversity, opportunistic user scheduling emerges as a proposed solution within the context of a multiuser HSTRN scenario, as discussed in An et al.'s [16] study. This scheduling strategy aims to optimize communication resources by opportunistically selecting users based on channel conditions and other relevant metrics, thereby enhancing overall network efficiency.

Furthermore, in the study of Upadhyay and Sharma [17], an in-depth investigation into HSTRN reveals benefits derived from a scheme incorporating both multi-user and multi-relay configurations. This holistic approach acknowledges the interconnectedness of multiple users and relays within the HSTRN system, emphasizing the potential for synergies that can be harnessed to improve communication reliability, coverage, and overall network performance. In summary, the standards IEEE 802.11s and IEEE 802.16j provide a solid foundation for the implementation of HSTRN functionalities. As the landscape of 5G mobile systems unfolds, the exploration of diverse applications within the HSTRN framework showcases its versatility and adaptability to meet the demands of modern communication scenarios.

On the other hand, cognitive radio technology (CR) addresses the challenge of spectrum utilization in wireless communication systems [18]. In CR networks, primary users (PUs) permit secondary users (SUs) universal access to signal transmission without compromising the quality of service (QoS) of the main network. Two primary techniques explored in CR networks include spectrum sharing and background spectrum reuse [19–21]. The spectrum-sharing model, in particular, does not impose strict restrictions on the transmission capacity of SUs. The integration of these models into satellite communications represents a significant improvement in the performance evaluation of next-generation wireless networks, offering enhancements in spectral efficiency, reduced error data connectivity, and broader coverage. In the research of Guo et al. [22], the performance of a STAR-RIS-empowered non-terrestrial vehicle network was investigated, where CR and non-orthogonal multiple access (NOMA) were utilized to enhance spectral efficiency (SE) and connectivity. Specifically, we derived the exact expressions for the outage probability (OP) for all secondary vehicle users, considering both imperfect and perfect successive interference cancellation (ipSIC and pSIC) in our proposed system. To gain further insights, we also provided the asymptotic outage probabilities at high signal-to-noise ratios (SNRs) and the diversity orders for all secondary vehicle users. In Liu et al.'s [23] research, a joint resource allocation strategy for a NOMA-enabled cognitive satellite-high altitude platform (HAP)-terrestrial network was investigated. The optimization problem was formulated as a mixed-integer nonlinear programming problem, characterized by its non-convexity and complexity. To tackle this challenging problem, the researchers decoupled it into two subproblems: subchannel allocation (SA) and power allocation (PA). For the SA subproblem, they designed a greedy heuristic algorithm to efficiently allocate subchannels. For the PA subproblem, they employed a successive convex approximation-based algorithm to optimize power distribution. Combining these approaches, they developed a joint resource allocation algorithm aimed at enhancing the performance of the proposed system. This method effectively balances the computational complexity and the optimization performance, providing a practical solution to the resource allocation problem in NOMA-enabled cognitive satellite-HAP-terrestrial networks. In the research of Liu et al. [24], the authors proposed a joint subchannel assignment and power allocation algorithm for NOMA-enabled cognitive satellite-unmanned aerial vehicle (UAV)-terrestrial networks to enhance transmission performance, taking into account imperfect channel state information.

While most current studies focus on the performance analysis of satellite systems [25–28], this paper takes inspiration from recent work in An et al. [25] and explores an OHSTCR system. Specifically, we evaluate the performance of the downlink communication scenario for ground users.

The remainder of this paper is organized as follows: Section 2 introduces the system model. Following that, section 3 provides an overview of the performance analysis of the primary network. In section 4, we present the numerical results and discussion. Finally, section 5 concludes the paper.

2. System model

Within the depicted system model illustrated in **Figure 1**, the OHSTCR system is intricately designed, incorporating both a primary satellite network and a secondary terrestrial network that coexist and share the same spectrum. The primary satellite, designated as 'O', is strategically positioned with the objective of transmitting a signal to a singular primary user (PU). In this configuration, the secondary transmitter (ST) node, denoted as 'U', engages in communication with its designated secondary receiver (SR), represented by 'V', leveraging spectrum access opportunities.

A noteworthy aspect of this system is the employment of amplify-and-forward (AF)-based relay cooperation within the ST. This cooperative relay mechanism is deployed to enhance and facilitate the primary transmission from the satellite to the primary user. The AF relay operation entails the ST amplifying the received signal and then forwarding it to the intended SR, contributing to the overall efficiency and reliability of the communication process.

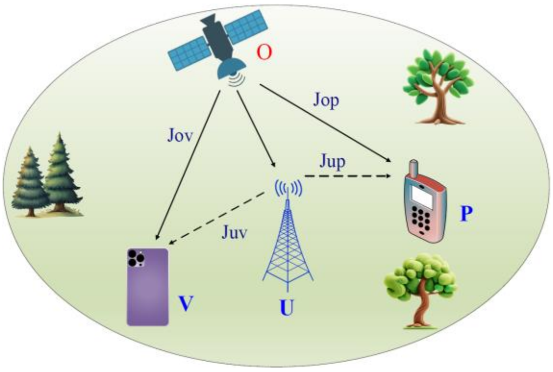

Figure 1. The OHSTCR system model.

In essence, this system architecture embodies a sophisticated interplay between satellite and terrestrial components, with the OHSTCR system orchestrating seamless communication between the primary satellite, primary user, and the secondary transmitter-receiver pair. The utilization of spectrum-sharing opportunities and the incorporation of relay cooperation mechanisms underscore the complexity and ingenuity embedded in the OHSTCR system, positioning it as a versatile and robust solution for efficient cognitive radio-based satellite-terrestrial communication. The channel coefficients corresponding to various links $O \to P$, $O \to U$, $O \to V$, $U \to P$, and $U \to V$ are represented by wireless channels j_{op}, j_{ou}, j_{ov}, j_{up}, and j_{uv}.

Satellite O transmits an information signal x_o (obeying $E[|x_o|^2] = 1$, where $E[.]$ denotes expectation) to many destinations.

$$y_{oi} = \sqrt{P_o} j_{oi} x_o + n_{oi} \quad (1)$$

where $i \in \{p, u, v\}$, P_o represents the transmit power at node O, and the term n_{oi} is the Additive Gaussian White Noise (AWGN). Node U can split its power to serve two directions.

$$z_u = \sqrt{\mu P_u} \frac{y_{ou}}{\sqrt{|y_{ou}|^2}} + \sqrt{(1-\mu) P_u} x_u \quad (2)$$

$\mu \in (0,1)$ stands for the power allocation factor. Therefore, the signals received at the respective nodes P and V, represented by y_{up} and y_{uv}, are given as:

$$y_{ul} = j_{ul} z_u + n_{ul} \quad (3)$$

where $l \in \{p, v\}$ and n_{ul} is the AWGN.

Considering the direct link $O \to P$, the end-to-end SNR at P is expressed by:

$$\Lambda_{op} = \eta_o |j_{op}|^2 \quad (4)$$

where $\eta_o = \frac{P_o}{\sigma^2}$. With regard to the relay link, the SNR at P and V can be computed respectively by:

$$\Lambda_{oup} = \frac{\mu \Lambda_{ou} \Lambda_{up}}{(1-\mu)\Lambda_{ou}\Lambda_{up} + \Lambda_{ou} + \Lambda_{up} + 1} \quad (5)$$

where $\Lambda_{ou} = \eta_o |j_{ou}|^2$, $\Lambda_{up} = \eta_u |j_{up}|^2$, and $\eta_u = \frac{P_u}{\sigma^2}$,

$$\Lambda_{ouv} = \frac{(1-\mu)\Lambda_{uv}(\Lambda_{ou} + 1)}{\mu \Lambda_{uv} + \Lambda_{ou} + 1} \quad (6)$$

where $\Lambda_{uv} = \eta_u |j_{uv}|^2$.

3. Performance analysis of the primary network

3.1. Characterizations of the channels

By applying Shadowed-Rician fading to the satellite links, the probability density function (PDF) of the channel gains $|j_{oi}|^2$, with $i \in \{p, u, v\}$, can be formulated as described in the study of An et al. [25].

$$f_{|j_{oi}|^2}(x) = \alpha_i e^{-\beta_x} {}_1F_1(m_{oi}; 1; \delta_i x), x \geq 0 \tag{7}$$

here, $\alpha_i = \left(2p_{oi}m_{oi}/(2p_{oi}m_{oi} + \Omega_{oi})\right)^{m_{oi}}/2p_{oi}$, $\beta_i = 1/2p_{oi}$, $\delta_i = \Omega_{oi}/(2p_{oi})(2p_{oi}m_{oi} + \Omega_{oi})$, where $2p_{oi}$ and Ω_{oi} represent the respective average powers of the multipath components and LOS, and m_{oi} denotes the fading severity parameter. $\Lambda_{oi} = \eta_o|j_{oi}|^2$ as detailed in the study of An et al. [25].

$$f_{\Lambda_{oi}}(x) = \alpha_i \sum_{k=0}^{m_{oi}-1} \frac{\zeta(k)}{(\eta_o)^{k+1}} x^k e^{-\left(\frac{\beta_i - \delta_i}{\eta_o}\right)x} \tag{8}$$

It is noted that $\zeta(k) = (-1)^k(1 - m_{oi})_k \delta_i^k/(k!)^2$, where $(.)_k$ represents the Pochhammer symbol. As such, the cumulative distribution function (CDF) $F_{\Lambda_{oi}}(x)$ can be derived by performing the integration of the PDF in Equation (8) as follows:

$$F_{\Lambda_{oi}}(x) = 1 - \alpha_i \sum_{k=0}^{m_{oi}-1} \frac{\zeta(k)}{(\eta_o)^{k+1}} \sum_{p=0}^{k} \frac{k!}{h!} \left(\frac{\beta_i - \delta_i}{\eta_o}\right)^{-(k+1-h)} \times x^h e^{-\left(\frac{\beta_i - \delta_i}{\eta_o}\right)x} \tag{9}$$

The channel gains $|j_{cl}|^2$ with $l \in \{p, v\}$ are assumed to follow the Gamma distribution with average power Ω_{ul} and fading severity m_{ul}. Hence, the PDF and CDF of $\Lambda_{ul} = \eta_u|j_{ul}|^2$ can be determined.

$$f_{\Lambda_{ul}}(x) = \left(\frac{m_{ul}}{\Omega_{ul}\eta_u}\right)^{m_{ul}} \frac{x^{m_{ul}-1}}{\Gamma(m_{ul})} e^{-\frac{m_{ul}}{\Omega_{ul}\eta_u}x} \tag{10}$$

and

$$F_{\Lambda_{ul}}(x) = \frac{1}{\Gamma(m_{ul})} \Upsilon\left(m_{ul}, \frac{m_{ul}}{\Omega_{ul}\eta_u} x\right) \tag{11}$$

here, $\Gamma(.)$ and $\Upsilon(.,.)$ represent, respectively, the complete gamma function and the lower incomplete gamma function, as detailed in the study of An et al. [25]: Equations (8.350.1) and (8.310.1).

3.2. Direct satellite transmission (DST)

Considering DST adopted at P, the outage probability (OP) of the primary network for a threshold rate R_h is computed by:

$$P_{out}^{DST}(R_h) = Pr\left[\log_2\left(1 + \Lambda_{op}\right) < R_h\right] \tag{12}$$

Alternatively, the OP can be further expressed as:

$$P_{out}^{DST}(R_h) = F_{\Lambda_{op}}(\gamma_h^{'}) \tag{13}$$

where $\gamma_h^{'} = 2^{R_h} - 1$.

Furthermore, to obtain the asymptotic OP, it can be approximated at high SNR as:

$$P_{out}^{DST}(R_h) \underset{\eta_o \to \infty}{\approx} \frac{\alpha_p}{\eta_o} \gamma_h^{'} \tag{14}$$

3.3. Cognitive radio with DST

In this scenario, the OP for the primary network in such a system is expressed as:

$$P_{out}^{DST}(R_h) = Pr\left[\frac{1}{2}\log_2\left(\Lambda_{op} + \Lambda_{oup}\right) < R_h\right] = Pr[\Lambda < \gamma_h] \tag{15}$$

where $\Lambda = \Lambda_{op} + \Lambda_{oup}$ and $\gamma_h = 2^{2R_h} - 1$.

$$P_{out}^{DST}(R_h) = \int_0^\infty F_\Lambda(\gamma_h|t) f_{Y_{ou}}(t)\mathrm{d}t \tag{16}$$

To solve Equation (16), we need to evaluate the conditional CDF, $F_\Lambda(\gamma_h|t)$, which can be expressed as:

$$F_\Lambda(\gamma_h|t) = Pr\left[\Lambda_{op} + \Lambda_{oup} < \gamma_h|t\right] = \int_0^{\gamma_h}\int_0^{\gamma_h - y} f_{\Lambda_{oup}}(\varphi|t) f_{\Lambda_{op}}(y)\mathrm{d}\varphi\mathrm{d}y \tag{17}$$

From Equation (17), by computing the CDF, $F_{\Lambda_{oup}}(\varphi|t)$, it is given as:

$$F_{\Lambda_{oup}}(\varphi|t) = Pr\left[\Lambda_{oup} < \varphi|t\right] = 1 - Pr\left[\Lambda_{oup} > \varphi|t\right] \tag{18}$$

Interestingly, the SNR expression for Λ_{oup} is rewritten as:

$$\Lambda_{oup} = \frac{1}{\left(\frac{1-\mu}{\mu}\right) + \frac{1}{\mu\Lambda_{ou}\Lambda_{up}}\left(\Lambda_{ou} + \Lambda_{up} + 1\right)} \tag{19}$$

Furthermore, in the high SNR regime, Equation (19) can be approximated as:

$$\Lambda_{oup} \approx \frac{1}{\xi + \frac{1}{\mu}\left(\frac{1}{\Lambda_{ou}} + \frac{1}{\Lambda_{up}}\right)} \tag{20}$$

where $\xi = \frac{1-\mu}{\mu}$. To calculate the OP, Equation (20) can be expressed as:

$$\Lambda_{oup} \approx \frac{1}{\xi + \frac{1}{\mu}\frac{1}{\min\left(\Lambda_{ou}, \Lambda_{up}\right)}} \tag{21}$$

Then, the asymptotic OP can be expressed as per [25]:

$$\begin{aligned} P_{out}^{asy}(R_z) \approx & \left[\sum_{i=0}^{M-1}\left\{\frac{\alpha_p}{\eta_o}\frac{i+1}{M}\gamma_h - \frac{\alpha_p}{\eta_o}\frac{i}{M}\gamma\right\}\right]\frac{\alpha_u}{\eta_o\varsigma(\gamma_h/M)} \\ & + \sum_{\substack{l=1\\M\geq 2}}^{M-1}\left[\sum_{i=0}^{M-l-1}\left\{\frac{\alpha_p}{\eta_o}\frac{i+1}{M}\gamma_h - \frac{\alpha_p}{\eta_o}\frac{i}{M}\gamma_h\right\}\right. \\ & \left. + \sum_{i=M-l}^{M-1}\left\{\frac{\alpha_p}{\eta_o}\frac{i+1}{M}\gamma_h - \frac{\alpha_p}{\eta_o}\frac{i}{M}\gamma_h\right\}\frac{1}{\Gamma(m_{up})m_{up}}\left(\frac{m_{up}}{\Omega_{up}\eta_u\varsigma\left(\frac{M-i}{M}\gamma_h\right)}\right)^{m_{up}}\right]\left(\frac{\alpha_u}{\eta_o\varsigma\left(\frac{l+1}{M}\gamma_h\right)}\right. \\ & \left. - \frac{\alpha_u}{\eta_o\varsigma\left(\frac{l}{M}\gamma_h\right)}\right) \\ & + \left[\sum_{i=0}^{M-1}\left\{\frac{\alpha_p}{\eta_o}\frac{i+1}{M}\gamma_h - \frac{\alpha_p}{\eta_o}\frac{i}{M}\gamma_h\right\}\frac{1}{\Gamma(m_{up})m_{up}}\left(\frac{m_{up}}{\Omega_{up}\eta_u\varsigma\left(\frac{M-i}{M}\gamma_h\right)}\right)^{m_{up}}\right]\left(1 - \frac{\alpha_u}{\eta_o\varsigma(\gamma_h)}\right) \end{aligned} \tag{22}$$

4. Numerical results and discussion

In this section, we set the main parameters as follows: $R_h = (0.1, 0.5, 1) bps/Hz$, $\gamma'_h = 0.414$, $\gamma_h = 1$, $\Omega_{up} = 1$, $m_{up} = 1$, $\eta_o = \eta_u = \eta$. It is noted that the satellite links $O \to P$ and $O \to U$ are subject to heavy shadowing (HS) with parameters as $(m_{op}, b_{op}, \Omega_{op} = 2, 0.063, 0.0005)$ and average shadowing (AS) with parameters as $(m_{ou}, b_{ou}, \Omega_{ou} = 5, 0.251, 0.279)$.

We are considering the OP performance of the primary user P.

In **Figure 2**, we observe a graphical representation of the OP in two primary network scenarios, portraying its variation with SNR. The discernible trend in the graph reveals a notable improvement in OP at elevated SNR levels. As SNR experiences an increase, there is a corresponding decrease in OP, indicating an enhancement in channel quality. This inverse relationship highlights the direct impact of signal strength on the operational performance of the network. Furthermore, the intricacies of OP are intricately tied to the target rate, as elucidated in the insights presented in **Figure 3**. The interplay between OP and the target rate unveils the nuanced constraints governing the network's operational efficiency. Moreover, **Figure 3** sheds light on the influence of the spectrum-sharing factor on OP, showcasing an observable correlation within the same visual representation. This comprehensive analysis not only deepens our understanding of the intricate dynamics of OP but also emphasizes the multifaceted factors influencing its performance within diverse network scenarios.

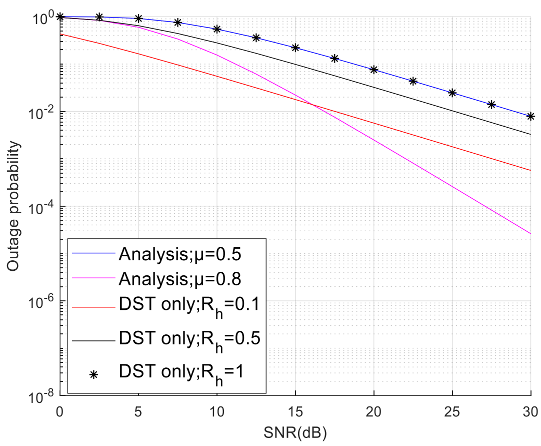

Figure 2. Outage performance versus SNR curves for primary network P under HS $(\mu = 0.5, \mu = 0.8, R_h = 0.1, R_h = 0.5, R_{\hbar} = 1)$.

Figures 4 and **5** provide insightful visual representations that elucidate the profound influence of SNR and the optimal values of the spectrum-sharing factor on the outage behavior within the examined network, specifically under HS and AS scenarios. The graphical depictions unveil compelling patterns and correlations, offering a deeper understanding of network dynamics.

Upon closer examination of **Figure 4**, it becomes apparent that higher SNR levels contribute substantially to a marked enhancement in OP. This implies that as the signal strength relative to the background noise increases, there is a consequential improvement in the network's ability to maintain operational reliability, thereby reducing the occurrence of outages. The graph serves as a visual testament to the pivotal role played by SNR in shaping the outage behavior of the network.

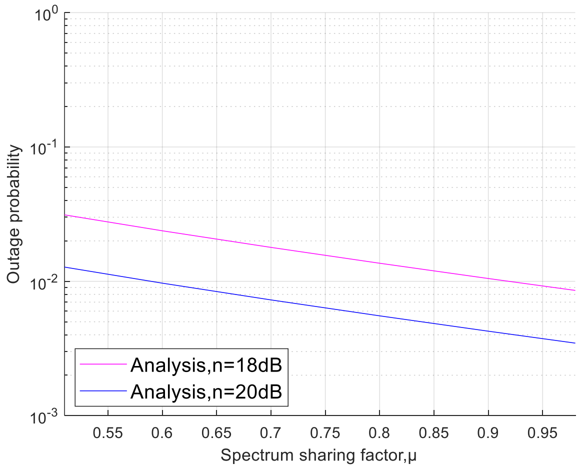

Figure 3. Outage performance versus μ curves for primary network P under HS ($\eta = 18$ dB, $\eta = 20$ dB).

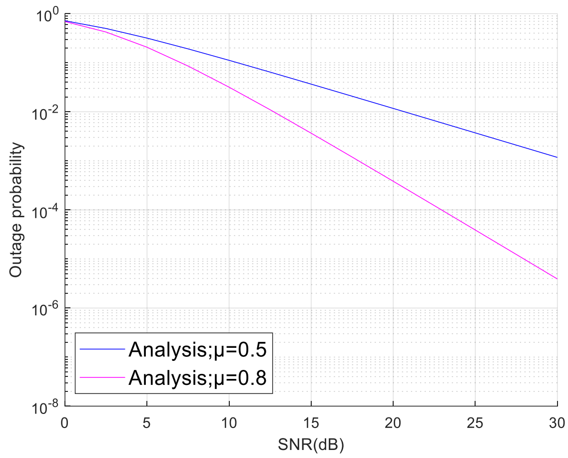

Figure 4. Outage performance versus SNR curves for primary network P under AS ($\mu = 0.5, \mu = 0.8$).

Simultaneously, **Figure 5** sheds light on the nuanced impact of the spectrum-sharing factor on OP. It becomes evident that while a high spectrum-sharing factor is at play, there is a discernibly modest alteration in OP. This indicates that the variability in the spectrum-sharing factor, while influential, does not induce drastic changes in the network's outage behavior. The figure underscores the importance of balancing considerations related to spectrum sharing, suggesting that its influence on OP is comparatively subtle in contrast to the more pronounced effects of SNR.

In summary, **Figures 4** and **5** collectively offer a comprehensive visual narrative that deepens our comprehension of the intricate interplay between SNR, spectrum-sharing factors, and outage behavior in the examined network scenarios. This nuanced analysis enhances our ability to make informed decisions and optimizations within the network architecture, considering both the impact of signal strength and spectrum-sharing parameters.

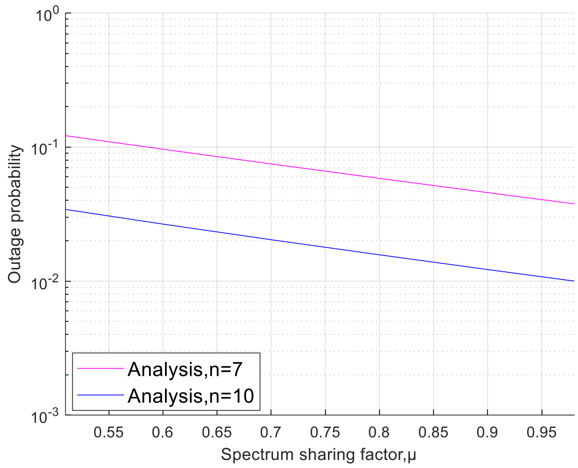

Figure 5. Outage performance versus SNR curves for primary network P under AS ($\eta = 7$ dB, $\eta = 10$ dB).

5. Conclusion

This paper systematically investigates the outage performance of an OHSTCR system, with the primary objective of guaranteeing optimal performance for users operating within a satellite network scenario. Within the realm of satellite communication, SNR and target rate have been identified as the predominant factors influencing the outage behavior experienced by ground users. The research goes a step further by delineating specific conditions that contribute to enhanced performance of the OHSTCR system. This involves meticulous control of key system parameters, illustrating how strategic adjustments can positively impact outage behavior and the overall reliability of the system. By presenting these conditions, the paper provides valuable insights for practitioners and researchers engaged in the design and implementation of CR systems tailored for satellite networks. The guidelines outlined in this paper serve as a practical roadmap for assisting in the design phase of CR systems within satellite network contexts. By placing particular emphasis on the manipulation of SNR and target rate, the paper not only contributes to a nuanced understanding of the factors influencing outage behavior but also offers actionable recommendations for optimizing system performance. In essence, these guidelines are crafted to aid in the development of CR systems that meet the stringent quality requirements for received signals on the ground, thereby elevating the overall efficacy and dependability of satellite communication networks. This research, therefore, stands as a valuable contribution to the field, offering actionable insights for the advancement of satellite-based cognitive radio systems.

Conflict of interest: The author declares no conflict of interest.

References

1. Li X, Wang Q, Peng H, et al. A Unified Framework for HS-UAV NOMA Networks: Performance Analysis and Location Optimization. IEEE Access. 2020; 8: 13329-13340. doi: 10.1109/access.2020.2964730
2. Evans B, Werner M, Lutz E, et al. Integration of satellite and terrestrial systems in future multimedia communications. IEEE Wireless Communications. 2005; 12(5): 72-80. doi: 10.1109/mwc.2005.1522108

3. Paillassa B, Escrig B, Dhaou R, et al. Improving satellite services with cooperative communications. International Journal of Satellite Communications and Networking. 2011; 29(6): 479-500. doi: 10.1002/sat.989
4. Sakarellos VK, Kourogiorgas C, Panagopoulos AD. Cooperative Hybrid Land Mobile Satellite–Terrestrial Broadcasting Systems: Outage Probability Evaluation and Accurate Simulation. Wireless Personal Communications. 2014; 79(2): 1471-1481. doi: 10.1007/s11277-014-1941-6
5. Chini P, Giambene G, Kota S. A survey on mobile satellite systems. International Journal of Satellite Communications and Networking. 2009; 28(1): 29-57. doi: 10.1002/sat.941
6. Bhatnagar MR, M.K. A. Performance Analysis of AF Based Hybrid Satellite-Terrestrial Cooperative Network over Generalized Fading Channels. IEEE Communications Letters. 2013; 17(10): 1912-1915. doi: 10.1109/lcomm.2013.090313.131079
7. Bhatnagar MR, Arti MK. Performance Analysis of Hybrid Satellite-Terrestrial FSO Cooperative System. IEEE Photonics Technology Letters. 2013; 25(22): 2197-2200. doi: 10.1109/lpt.2013.2282836
8. Javed U, He D, Liu P. Performance Characterization of a Hybrid Satellite-Terrestrial System with Co-Channel Interference over Generalized Fading Channels. Sensors. 2016; 16(8): 1236. doi: 10.3390/s16081236
9. Lin M, Ouyang J, Zhu WP. On the performance of hybrid satelliteterrestrial cooperative networks with interferences. In: Proceedings of the 48th Asilomar Conf. Signals, Syst. Comput. (ACSSC); November 2014; Pacific Grove, CA, USA. pp. 1796-1800.
10. Yang L, Hasna MO. Performance Analysis of Amplify-and-Forward Hybrid Satellite-Terrestrial Networks with Cochannel Interference. IEEE Transactions on Communications. 2015; 63(12): 5052-5061. doi: 10.1109/tcomm.2015.2495278
11. Sreng S, Escrig B, Boucheret ML. Exact Symbol Error Probability of Hybrid/Integrated Satellite-Terrestrial Cooperative Network. IEEE Transactions on Wireless Communications. 2013; 12(3): 1310-1319. doi: 10.1109/twc.2013.013013.120899
12. An K, Ouyang J, Lin M, et al. Outage Analysis of Multi-Antenna Cognitive Hybrid Satellite-Terrestrial Relay Networks With Beamforming. IEEE Communications Letters. 2015; 19(7): 1157-1160. doi: 10.1109/lcomm.2015.2428256
13. An K, Lin M, Ouyang J, et al. Symbol Error Analysis of Hybrid Satellite–Terrestrial Cooperative Networks With Cochannel Interference. IEEE Communications Letters. 2014; 18(11): 1947-1950. doi: 10.1109/lcomm.2014.2361517
14. Hemachandra KT, Beaulieu NC. Outage Analysis of Opportunistic Scheduling in Dual-Hop Multiuser Relay Networks in the Presence of Interference. IEEE Transactions on Communications. 2013; 61(5): 1786-1796. doi: 10.1109/tcomm.2013.031213.120686
15. Erwu L, Dongyao W, Jimin L, et al. Performance evaluation of bandwidth allocation in 802.16j mobile multi-hop relay networks. In Proceedings of the IEEE VTC-Spring; April 2007; Dublin, Ireland. pp. 939-943.
16. An K, Lin M, Liang T. On the Performance of Multiuser Hybrid Satellite-Terrestrial Relay Networks with Opportunistic Scheduling. IEEE Communications Letters. 2015; 19(10): 1722-1725. doi: 10.1109/lcomm.2015.2466535
17. Upadhyay PK, Sharma PK. Max-Max User-Relay Selection Scheme in Multiuser and Multirelay Hybrid Satellite-Terrestrial Relay Systems. IEEE Communications Letters. 2016; 20(2): 268-271. doi: 10.1109/lcomm.2015.2502599
18. Haykin S. Cognitive radio: brain-empowered wireless communications. IEEE Journal on Selected Areas in Communications. 2005; 23(2): 201-220. doi: 10.1109/jsac.2004.839380
19. Zou Y, Zhu J, Zheng B, et al. An Adaptive Cooperation Diversity Scheme with Best-Relay Selection in Cognitive Radio Networks. IEEE Transactions on Signal Processing. 2010; 58(10): 5438-5445. doi: 10.1109/tsp.2010.2053708
20. Han Y, Pandharipande A, Ting SH. Cooperative decode-and-forward relaying for secondary spectrum access. IEEE Transactions on Wireless Communications. 2009; 8(10): 4945-4950. doi: 10.1109/twc.2009.081484
21. Manna R, Louie RHY, Yonghui Li, et al. Cooperative Spectrum Sharing in Cognitive Radio Networks with Multiple Antennas. IEEE Transactions on Signal Processing. 2011; 59(11): 5509-5522. doi: 10.1109/tsp.2011.2163068
22. Guo K, Liu R, Alazab M, et al. STAR-RIS-Empowered Cognitive Non-Terrestrial Vehicle Network With NOMA. IEEE Transactions on Intelligent Vehicles. 2023; 8(6): 3735-3749. doi: 10.1109/tiv.2023.3264212
23. Liu R, Guo K, An K, et al. Resource Allocation for Cognitive Satellite-HAP-Terrestrial Networks With Non-Orthogonal Multiple Access. IEEE Transactions on Vehicular Technology. 2023; 72(7): 9659-9663. doi: 10.1109/tvt.2023.3252642
24. Liu R, Guo K, An K, et al. Resource Allocation for NOMA-Enabled Cognitive Satellite-UAV-Terrestrial Networks With Imperfect CSI. IEEE Transactions on Cognitive Communications and Networking. 2023; 9(4): 963-976. doi: 10.1109/tccn.2023.3261311
25. An K, Lin M, Zhu WP, et al. Outage Performance of Cognitive Hybrid Satellite–Terrestrial Networks With Interference

Constraint. IEEE Transactions on Vehicular Technology. 2016; 65(11): 9397-9404. doi: 10.1109/tvt.2016.2519893

26. Shi S, Li G, An K, et al. Optimal power control for real-time applications in cognitive satellite terrestrial networks. IEEE Commun. Lett. 2017; 21(8): 1815-1818.
27. Kolawole OY, Vuppala S, Sellathurai M, et al. On the Performance of Cognitive Satellite-Terrestrial Networks. IEEE Transactions on Cognitive Communications and Networking. 2017; 3(4): 668-683. doi: 10.1109/tccn.2017.2763619
28. Singh V, Solanki S, Upadhyay PK. Cognitive Relaying Cooperation in Satellite-Terrestrial Systems with Multiuser Diversity. IEEE Access. 2018; 6: 65539-65547. doi: 10.1109/access.2018.2877130